# Scaled interfacial activity of proteins at a hydrophobic solid/aqueous-buffer interface

**Anandi Krishnan,[1] Yi-Hsiu Liu,[2] Paul Cha,[2] David Allara,[2,3] Erwin A. Vogler[1,2]**
[1]*Department of Bioengineering, The Pennsylvania State University, University Park, PA 16802*
[2]*Department of Materials Science and Engineering, The Pennsylvania State University, University Park, PA 16802*
[3]*Department of Chemistry, The Pennsylvania State University, University Park, PA 16802*

Received 2 November 2004; revised 8 April 2005; accepted 21 April 2005
Published online 15 August 2005 in Wiley InterScience (www.interscience.wiley.com). DOI: 10.1002/jbm.a.30444

**Abstract:** Contact-angle goniometry confirms that interfacial energetics of protein adsorption to the hydrophobic solid/aqueous-buffer (solid–liquid, SL) surface is not fundamentally different than adsorption to the aqueous-buffer/air (liquid–vapor, LV) interface measured by pendant-drop tensiometry. Adsorption isotherms of 9 globular blood proteins with molecular weight (MW) spanning from 10 to 1000 kDa on methyl-terminated self-assembled monolayer surfaces demonstrate that (i) proteins are weak surfactants, reducing contact angles by no more than about 15° at maximum solution concentrations (~10 mg/mL); (ii) the corresponding dynamic range of spreading pressure $\Pi_a < 20$ m$N$/m; and (iii) the maximum spreading pressure $\Pi_a^{max}$ for these diverse proteins falls within a relatively narrow 5 m$N$/m band. As with adsorption to the LV interface, we find that concentration scaling substantially alters perception of protein interfacial activity measured by $\Pi_a$. Proteins appear more similar than dissimilar on a weight/volume basis whereas molarity scaling reveals a systematic ordering by MW, suggesting that adsorption is substantially driven by solution concentration rather than diversity in protein amphilicity. Scaling as a ratio-to-physiological-concentration demonstrates that certain proteins exhibit $\Pi_a^{max}$ at-and-well-below physiological concentration whereas others require substantially higher solution concentration to attain $\Pi_a^{max}$. Important among this latter category of proteins is blood factor XII, assumed by the classical biochemical mechanism of plasma coagulation to be highly surface active, even in the presence of overwhelming concentrations of other blood constituents such as albumin and immunoglobulin that are shown by this work to be among the class of highly surface-active proteins at physiologic concentration. The overarching interpretation of this work is that water plays a dominant, controlling role in the adsorption of globular-blood proteins to hydrophobic surfaces and that energetics of hydration control the amount of protein adsorbed to poorly water-wettable biomaterials. © 2005 Wiley Periodicals, Inc. J Biomed Mater Res 75A: 445–457, 2005

**Key words:** protein adsorption; hydrophobic solid–liquid interface; blood proteins; FXII; coagulation; SAM

## INTRODUCTION

The protein adsorption problem — how (glyco)proteins selectively collect at biomaterial surfaces from complex solutions such as blood; the structure–property relationships connecting surface chemistry/energy to the extent and specificity of protein adsorption; and the manner by which surface-bound protein directs biological responses such as blood coagulation, cell/tissue adherence, or fouling of medical devices — remains one of the quintessential unsolved mysteries of biomaterials surface science. And yet a full understanding of protein adsorption is essential to prospective, fundamentals-driven design of biomaterials. This is because protein adsorption is among the first molecular-level interactions with a biomaterial that ultimately lead to biocompatibility, or lack thereof (see, for example, Refs. 1–5 and citations therein).

Our work probing each of the above aspects of the protein adsorption problem strongly implicates water as a moderating or mediating agent.[6–10] We have pursued the long-standing hypothesis that surface interactions with water and reorganization of ions near the water-contacting surface precede protein adsorption,[11] forming a hydration layer extending some (generally unknown) distance from the water-contacting surface with which protein molecules interact.[10] This layer is variously referred to as bound water[12–14]

*Correspondence to*: E. A. Vogler; e-mail: eav3@psu.edu
Contract grant sponsor: National Institute of Health; contract grant number: PHS 1 R01 HL 69965-03
Contract grant sponsor: Johnson & Johnson Focused Giving Grant Program
Contract grant sponsor: Materials Research Institute and Departments of Bioengineering and Materials Science and Engineering, Pennsylvania State University

or vicinal water[6,15] or as an interphase,[16,17] depending on the context and application. However termed, we find that vicinal water controls protein adsorption to surfaces by resisting displacement with adsorbing protein molecules. In turn, resistance to displacement depends on the affinity of water for the surface,[10,17] and so protein adsorption is found to scale with surface energy (water wettability).[18–20] According to this view, water-wettable surfaces (a.k.a., hydrophilic)[21] with strongly bound vicinal water adsorb little-or-no protein directly onto the surface; although this does not necessarily rule out collection of protein near the surface in a manner that does not require dehydration of the surface.[6,10,22–24] By contrast, proteins can adsorb directly onto poorly water-wettable (hydrophobic) surfaces by displacing relatively weakly bound vicinal water.[18–20]

Detailed examination of these basic principles operating at the aqueous-buffer/air (liquid–vapor, LV) interface, a molecularly smooth hydrophobic surface, strongly suggests that water does indeed orchestrate a clearly discernable, systematic pattern in protein adsorption.[25] Specifically, we find that: (i) variation in globular blood protein amphilicity (interaction energetics with water) with composition spanning three decades of molecular weight (MW) is surprisingly modest; (ii) the equilibrium partition coefficient $P$ (ratio of interphase-to-bulk concentration) is relatively constant across this diverse group of proteins $10^2 < P < 10^3$with $P \sim 150$ taken as nominal value); (iii) interphase capacity for protein is limited by the extent to which the LV surface can be dehydrated by displacement of interfacial water by adsorbing protein; and that (iv) molar concentrations required to fill the LV interphase follow a homology in protein size consistent with packing hydrated spheroidal molecules within this space.[16] This latter effect is particularly interesting because it predicts that molar-interphase concentrations scale inversely with protein MW and, as a consequence, multiple layers of higher-MW proteins (MW $>$ 125 kDa) are required to fully fill the LV surface. For example, one molecular layer of albumin (MW = 66.3 kDa) is predicted to fully saturate the LV surface whereas two layers of IgG (MW = 160 kDa) are required (both of which have been confirmed experimentally),[26,27] and five layers of IgM (MW = 1000 kDa) form at the saturated LV surface[16] (which apparently awaits experimental verification).

It turns out that fixed LV surface capacity for protein at approximately constant $P$ imposes significant constraints on the protein adsorption problem. That is to say, because protein adsorption is more about solvent than adsorbate, a tractable quasi-thermodynamic theory describes a phenomenon that would otherwise be overwhelmingly complex for more than just a few proteins in solution. In fact, a straightforward set of mixing rules stipulates both concentration and weight-fraction distribution of proteins adsorbed to the LV interphase from multi-component aqueous solutions such as blood plasma or serum at equilibrium.[28] These mixing rules rationalize the long-known but otherwise unexplained observations that (i) LV interfacial tension $\gamma_{lv}$ of blood plasma and serum is nearly identical, in spite of the fact that serum is substantially depleted of coagulation proteins such as fibrinogen; and (ii) $\gamma_{lv}$ of plasma and serum derived from human, bovine, ovine, and equine blood is practically identical, even though there are substantial differences in the plasma proteome among these species.[29] Thus, in summary, we find that protein adsorption to the LV surface, including certain aspects of the Vroman effect,[28] can be quite well understood on the basis of the behavior of water at surfaces.

This article discloses results of an investigation of protein adsorption to a well-defined, hydrophobic solid/aqueous-buffer (solid–liquid, SL) interface. Methyl-terminated self-assembled thiol monolayers (SAMs) on gold-coated semiconductor-grade silicon wafers exhibiting water contact angles $\theta_a \sim 100°$ are used as test substrata. Time- and concentration-dependent contact angles are used to measure adsorption energetics of (globular) proteins spanning three decades in MW in a manner that parallels the above-cited studies of protein adsorption to the LV surface. We find that the basic pattern observed at the LV surface is repeated at the hydrophobic SL surface, supporting our contention that water is the significant controller of protein adsorption to biomaterial surfaces.

## MATERIALS AND METHODS

### Purified proteins and synthetic surfactants

Table I compiles pertinent details on proteins and surfactants used in this work. Protein purity was certified by the vendor to be no less than the respective values specified in column 4 of Table I, as ascertained by electrophoresis (SDS-PAGE or IEP). Mass, concentration, and molecular weights supplied with purified proteins were accepted without further confirmation. Issues associated with protein purity, especially contamination with surfactants, and the potential effect on measured interfacial tensions were discussed in detail in Ref. 25. The single value given in Table I for physiological concentration of human proteins (column 5) applied in this work was middle of the range listed by Putnam.[30] Serial dilutions of protein stock solutions (usually 10 mg/mL) were performed in 96-well microtiter plates by (typically) 50:50 dilution in phosphate-buffered saline solution (0.01*M* PBS, 0.14*M* NaCl, 0.003*M* KCl) prepared from powder (Sigma Aldrich) in distilled-deionized (18 MΩ) water using pro-

**TABLE I**
**Purified Proteins and Surfactants**

| Name of Protein/Surfactant (acronym) | | Molecular Weight (kDa) | As Received Form (mg/mL) | Purity (electrophoresis) or Activity | Physiologic Concentration mg/100 mL (nominal value) | Vendor |
|---|---|---|---|---|---|---|
| Ubiquitin (Ub) | Prep 1 | 10.7 | Powder | 98% | 10–20 (15) | Sigma Aldrich |
| | Prep 2 | | | 95% | | EMD Biosciences |
| Thrombin (FIIa) | | 35.6 | Powder | 1411 NIH units/mg | N/A | Sigma Aldrich |
| Human serum albumin Fraction V (FV HSA) | Prep 1 | 66.3 | Powder | 98% | 3500–5500 (4500) | MP Biomedicals |
| | Prep 2 | | Powder | 98% | | |
| Prothrombin (FII) | | 72 | Powder | 7.5 units/mg protein | 5–10 (7.5) | Sigma Aldrich |
| Factor XII (FXII) | Prep 1 | 78 | Solution (2.1) | 95% | (4) | Hematologic Technologies |
| | Prep 2 | | Solution (5.5) | | | |
| Human IgG (IgG) | | 160 | Powder | 97% | 800–1800 (1300) | Sigma Aldrich |
| Complement component CIq (CIq) | | 400 | Solution (1.1) | Single band by immunoelectrophoresis | 10–25 (17.5) | Sigma Aldrich |
| $\alpha_2$-macroglobulin ($\alpha$mac) | Prep 1 | 725 | Powder | 98% | 150–350 (250) | Sigma Aldrich |
| | Prep 2 | | | | | Sigma Aldrich |
| | Prep 3 | | | | | MP Biomedicals |
| Human IgM (IgM) | Prep 1 | 1000 | Solution (0.8) | 98% | 60–250 (155) | Sigma Aldrich |
| | Prep 2 | | Solution (5.1) | Single band by immunoelectrophoresis | | MP Biomedicals |
| Sodium dodecyl sulfate (SDS) | | 0.28 | Powder | N/A | N/A | Sigma Aldrich |
| Tween 20 (TWN20) | | 1.23 | Neat | N/A | N/A | Sigma Aldrich |

cedures detailed in Ref. 25 (interfacial tension of PBS and water was checked periodically by Wilhelmy-balance tensiometry). Between 24 and 30 dilutions were prepared in this manner, covering a dynamic range between $10^{-10}$ to 1 % (w/v), taking care to mix each dilution by repeated pipette aspiration and avoiding foaming of concentrated solutions.

## Surfaces

Methyl-terminated self assembled monolayer surfaces (SAMs) were prepared according to standard methods of surface engineering. Details involved have been reported elsewhere.[31–35] Alkanethiol (Aldrich Chemical Co., Milwaukee, WI) and ethanol (commercial reagent grade) were used as received, without further purification. Samples were stored in the thiol solution until use, and were rinsed with ethanol just prior to an experiment.

## Tensiometry and goniometry

Liquid–vapor interfacial tensions required by this work were measured by pendant drop tensiometry (PDT) as described in Refs. 16, 25, 28, 29. Contact angle and wettability methods applied in this work have been disclosed in detail elsewhere, including verification that measured advancing angles ($\theta_a$) were in statistical agreement with that obtained by Wilhelmy balance tensiometry.[36,37] Receding angles ($\theta_r$) were shown to be not as reliable as $\theta_a$. Consequently, only $\theta_a$ was analyzed in this work. Briefly, for the purposes of this paper, $\theta_a$ measurements were made using a commercial automated tilting-plate goniometer (TPG, First Ten Angstroms Inc., Portsmouth VA). The goniometer employed a Tecan liquid-handling robot to aspirate 12 $\mu$L of solutions contained in a 96-well microtiter plate prepared by the serial-dilution protocol mentioned above. We found that dip coating of disposable polypropylene tips in a commercial perfluorocarbon hydrophobizing agent (NYEBAR, NYE

Lubricants Inc., Bedford, MA) followed by water wash and air drying greatly aided dispensing of drops, especially at the highest protein concentrations (lowest $\gamma_{lv}$). This coating procedure was shown not to measurably affect interfacial tensions or contact angles. The robot was used to reproducibly transfer the tip with fluid contents into a humidified (99+ % RH) analysis chamber and dispense 10 μL drops of protein solution onto the surface of test substrata (see below) held within the focal plane of a magnifying camera. These and all other aspects of tilting-plate goniometry were performed under computer control. Proprietary algorithms supplied by the vendor were used to deduce contact angles from drop images captured at a programmed rate by a frame grabber. Typically, 600 images were captured at a rate of 1 image every 6 s following 0.25-s delay to permit vibrations of the expelled drop to dampen. Drop evaporation rates within the humidified chamber deduced from computed-drop volumes (based on image analysis) were observed to vary with solute concentration, generally ranging from approximately 25 nL/min for pure water to 10 nL/min for solute solutions $> 0.1\%$ w/v. The impact of this evaporation rate over the 60 min time frame of the experiment was apparently negligible, as gauged from the behavior of purified surfactants discussed in the results section and in Ref. 37. Precision of $\theta_a$ was about 0.5° based on repeated measurement of the same drop. The analysis chamber was thermostated to a lower-limit of 25 ± 1°C by means of a computer-controlled resistive heater. Upper-temperature limit was not controlled but rather floated with laboratory temperature, which occasionally drifted as high as 29°C during summer months. Thus, reported $\theta_a$ values were probably not more accurate than about 1° on an intersample basis considering the small, but measurable, variation of water interfacial tension with temperature. This range of accuracy was deemed adequate to the conclusions of this report which do not strongly depend on more highly accurate $\theta_a$ that is difficult to achieve on a routine basis. Instead, veracity of arguments raised herein depend more on a breadth of reliable measurements made across the general family of human proteins.

Test substrata were held on a rotating, tilting-plate platform driven by stepper motors under computer control. Substrata were allowed to come to equilibrium within the sample-chamber environment for no less than 30 min before contact angle measurements were initiated. The platform was programmed to tilt at 1°/s from horizontal to 25° after the drop was deposited on the surface by the robot. The optimal (incipient rolling) tilt angle was found to be 25° and 15° for solutions of proteins and surfactants, respectively. The first 120 s (20 images) monitored evolution of the advancing angle. At the end of the 1 h, $\theta_a$ measurement period, the platform was programmed to return to horizontal and rotate 15° to the next analysis position along the periphery of the semiconductor wafer. This process was repeated for all dilutions of the protein under study so that results reported for each protein were obtained on a single test surface, eliminating the possibility of substratum-to-substratum variation within reported results. We observed that the contact angle of a pure PBS droplet slowly decreased with time from the initial value of $108° < \theta_a < 106°$ at t = 0 to $104° < \theta_a^{\circ} < 102°$ at t = 1 h; where $\theta_a^{'}$ (see Fig. 1 for examples). Successive no-linear least-squares fitting of a four-parameter logistic equation $[\theta_a = \theta^{\circ}_a - \theta'_a / 1 + (\ln C_B^{\theta/2} / \ln C_B)^M + \theta'_a]$ to contact angle isotherms data for each time within the observation interval quantified $\theta_a$ and $\theta_a^{'}$ parameters with a measure of statistical uncertainty. Fitting also recovered a parameter measuring concentration-at-half-maximal-change in $\theta_a$, $\ln C_B^{\Theta/2}$ where $\Theta/2 = 1/2\Theta^{max}$ and $\Theta^{max} \equiv \theta^{\circ}_a - \theta'_a$) as well as a parameter *M* that measured steepness of the sigmoidal curve. This multi-parameter fitting to concentration-dependent $\theta_a$ data was a purely pragmatic strategy that permitted quantification of best-fit protein and surfactant characteristics but is not a theory-based analysis.[17–19] Three-dimensional (3D) representations of time-and-concentration $\theta_a$ data were created in Sigma Plot (v8) from the data matrix discussed above and overlain onto fitted-mesh data computed from least-squares fitting. Two-dimensional (2D) representations were created from the same data matrices at selected observation times. Measured $\theta_a$ were converted to advancing adhesion tension $\tau_a = \gamma_{lv} \cos\theta_a$ for general interpretation[17]; where $\gamma_{lv}$ is the interfacial tension of the contact-angle fluid. Adhesion tensions $\tau^{\circ}_a = \gamma^{\circ}_{lv} \cos\theta^{\circ}_a$ (pure saline) and $\tau_a' = \gamma_{lv}' \cos\theta_a'$ (at the minimum contact angle observed $\theta_a$) were computed with fitted parameters $\gamma_{lv}^{\circ}$ and $\gamma_{lv}^{'}$ reported in Ref. 25 for the

**Figure 1.** Contact angle isotherms in 3D [$\theta_a$ as a function of analysis time (drop age) and logarithmic (natural) solution concentration $C_B$] and 2D ($\theta_a$ as a function of logarithmic solution concentration $C_B$ at selected times) formats comparing sodium dodecyl sulfate (SDS, panel A), human serum albumin (FV HSA, panel B, preparation 1, Table II), and $\alpha_2$-macroglobulin (panel C, preparation 1, Table II). In each case, solute concentration $C_B$ is expressed in picomoles/L (p*M*) on a natural logarithmic scale. Symbols in 2D panels represent time slices through 3D representations (filled circle, 0.25 s; open circle, 900 s; filled triangles, 1800 s; open triangles, 3594 s; annotations in panel A indicate maximum and half-maximum contact angle reduction). Notice that adsorption kinetics dominated $\alpha_2$-macroglobulin adsorption whereas steady state was achieved within about 1000 s for HSA, and nearly no adsorption kinetics is detected for SDS. Note also decrease in $\theta_a^{\circ}$ with time, attributed to slow hydration of the SAM surface (arrow annotation, panel B; see Results section).

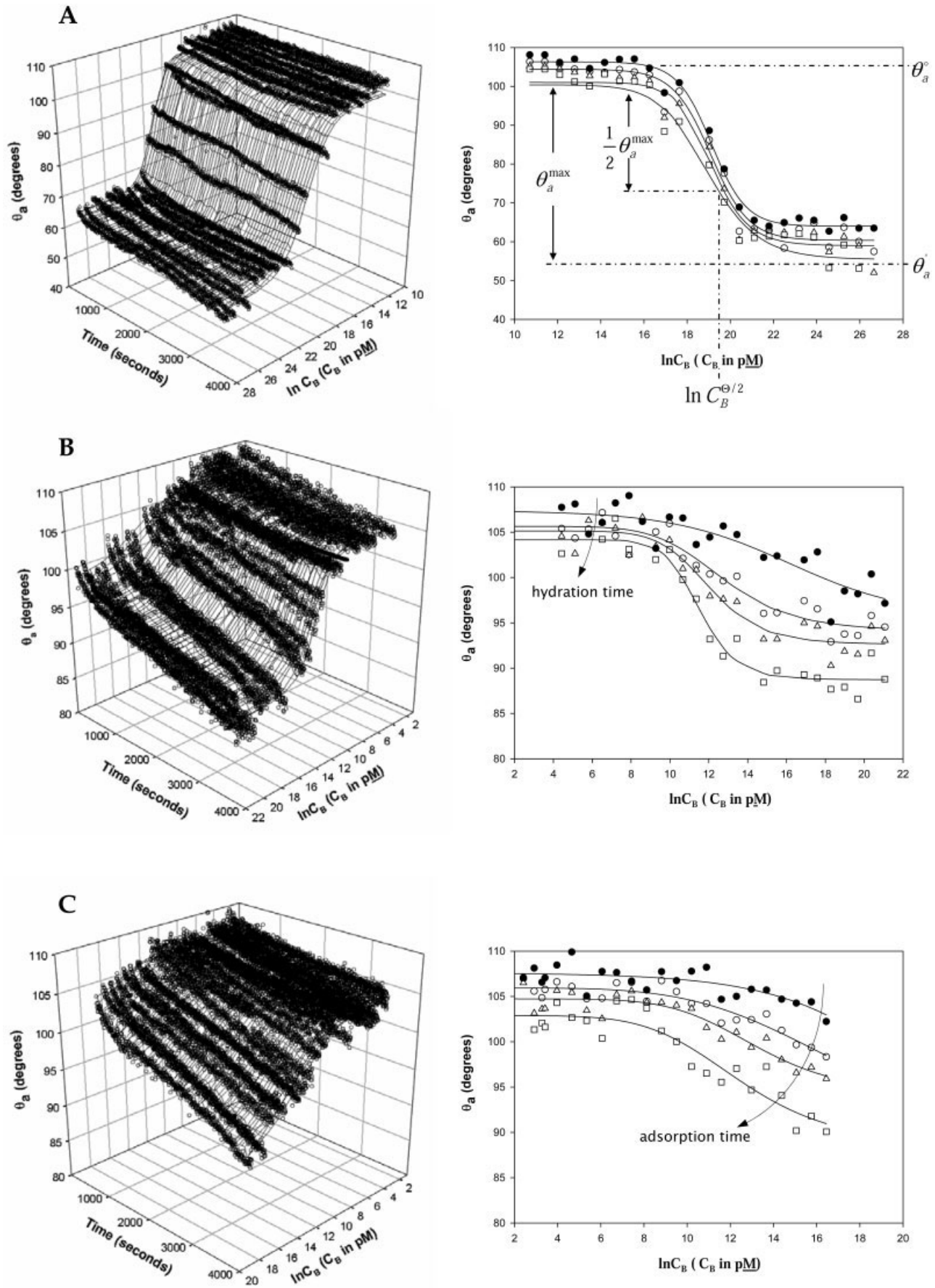
A
θa (degrees)
Time (seconds)
ln CB (CB in pM)
lnCB ( CB in pM)
B
hydration time
C
adsorption time

**Figure 1.**

**TABLE II**
**Steady-state Protein Adsorption Parameters**

| Name of Protein/Surfactant (acronym) | | $\theta_a^\circ$ (degrees) | $\theta_a'$ (degrees) | $\ln C_B^{\theta/2}$ PPT (p*M*) | M (dimensionless) | $\tau_a^\circ$ (m*N*/m) | $\tau_a'$ (m*N*/m) | $\Pi_a^{max}$ (m*N*/m) | $\ln C_B^{max}$ (p*M*) |
|---|---|---|---|---|---|---|---|---|---|
| Ubiquitin (Ub)* | Prep 1 | 100.9 ± 0.5 | 75 | 19 (17) | — | −14 | 7 | 21 | 19 |
| | Prep 2 | 102.2 ± 0.9 | 75 | 19 (17) | — | −15 | 12 | 27 | 19 |
| | | | | 17.5 ± 0.2 | | | | | |
| Thrombin (FIIa) | | 99.8 ± 0.5 | 84.6 ± 0.9 | (13.9 ± 0.2) | −25.0 ± 8.5 | −12.3 ± 0.6 | 4.5 ± 0.7 | 16.7 ± 0.9 | 15.1 ± 0.2 |
| Human serum albumin FV HSA | | | | 15.9 ± 0.3 | | | | | |
| | Prep 1 | 103.3 ± 0.8 | 88.3 ± 0.8 | (11.7 ± 0.3) | −14.1 ± 5.7 | −16.3 ± 0.9 | 1.4 ± 0.6 | 17.7 ± 1.2 | 13.6 ± 0.3 |
| | | | | 15.7 ± 0.3 | | | | | |
| | Prep 2 | 104.5 ± 0.8 | 88.5 ± 0.6 | (11.5 ± 0.3) | −11.6 ± 3.0 | −17.7 ± 0.9 | 1.2 ± .5 | 18.9 ± 1.1 | 13.7 ± 0.3 |
| | | | | 15.1 ± 0.4 | | | | | |
| Prothrombin (FII) | | 100.6 ± 0.5 | 86.5 ± 0.9 | (10.8 ± 0.4) | −10.1 ± 2.7 | −12.9 ± 0.6 | 2.6 ± 0.7 | 15.6 ± 0.9 | 13.2 ± 0.4 |
| | | | | 15.6 ± 0.5 | | | | | |
| Factor XII* | Prep 1 | 102.9 ± 0.5 | 94.8 ± 1.0 | (11.3 ± 0.5) | −17.9 ± 1.2 | −15.6 | −3.1 | 12.5 | 12.7 ± 0.5 |
| | | | | 15.7 ± 0.4 | | | | | |
| | Prep 2 | 102.0 ± 0.4 | 88.2 ± 0.8 | (11.3 ± 0.4) | −10.9 ± 3.3 | −14.6 | 1.2 | 15.8 | 13.6 ± 0.4 |
| | | | | 15.1 ± 0.9 | | | | | |
| Human IgG (IgG) | | 103.7 ± 0.7 | 94.9 ± 1.4 | (10.1 ± 0.9) | −6.9 ± 4.7 | −16.8 ± 0.9 | −4.4 ± 1.3 | 12.4 ± 1.5 | 13.3 ± 0.9 |
| Complement component C1q (C1q) | | | | 15.6 ± 0.4 | | | | | |
| | | 102.6 ± 0.4 | 95.3 ± 0.7 | (9.6 ± 0.4) | −12.1 ± 5.6 | −15.6 ± 0.5 | −5.0 ± 0.7 | 10.6 ± 0.8 | 11.4 ± 0.4 |
| $\alpha_2$-macroglobulin* ($\alpha$ mac) | Prep 1 | 101.9 ± 0.5 | 86 | 19 (13) | — | −15 | 4 | 19 | 17 |
| | Prep 2 | 100.2 ± 0.9 | | | | | | | |
| | Prep 3 | 103.2 ± 0.5 | | | | | | | |
| | | | | 15.5 ± 0.5 | | | | | |
| Human IgM (IgM) | Prep 1 | 102.7 ± 0.6 | 91.3 ± 1.6 | (8.7 ± 0.5) | −7.4 ± 2.9 | −15.7 ± 0.7 | −1.1 ± 1.4 | 14.6 ± 1.6 | 11.3 ± 0.5 |
| | | | | 15.9 ± 0.6 | | | | | |
| | Prep 2 | 102.4 ± 0.6 | 87.8 ± 2.0 | (9.2 ± 0.7) | −4.9 ± 1.6 | −15.4 ± 0.7 | 1.9 ± 1.7 | 17.3 ± 1.9 | 12.6 ± 0.8 |
| Sodium dodecyl sulfate (SDS) | | | | 17.7 ± 0.4 | | | | | |
| | | 100.1 ± 1.9 | 56.0 ± 2.3 | (18.9 ± 0.4) | −17.3 ± 4.6 | −12.5 ± 2.3 | 18.7 ± 1.1 | 31.2 ± 2.6 | 21.4 ± 0.4 |
| | | | | 16.4 ± 0.3 | | | | | |
| Tween 20 (TWN20) | | 97.1 ± 0.6 | 65.1 ± 0.7 | (16.2 ± 0.1) | −23.4 ± 3.3 | −8.9 ± 0.8 | 14.6 ± 0.5 | 23.5 ± 0.6 | 17.8 ± 0.1 |

*Parameters are graphical estimates of fitted parameters. See Results section.

proteins under investigation. Smoothed adhesion–tension isotherms ($\tau_a$ vs. $\ln C_B$) were computed from smoothed $\theta_a$ obtained from $\theta_a$ isotherms above, using smoothed $\gamma_{lv}$ values computed from best-fit parameters reported in Ref. 25. Likewise, smoothed spreading pressure isotherms ($\Pi_a$ vs.$\ln C_B$) were computed from smoothed $\tau_a$ curves where $\Pi_a = \tau_a - \tau_a^\circ$.

## RESULTS AND DISCUSSION

Results and discussion are combined into one section because it is efficient to introduce and discuss the different facets of the work in the sequence that follows and then combine separate observations in the Conclusions section. The presentation follows the basic outline used in a companion paper published in this journal describing protein adsorption to the LV surface.[25] First, general characteristics of the quantitative data are described, comparing proteins to a surfactant reference compound and placing data into an overall context for interpretation. Results are then interpreted graphically by scaling concentration-dependent SL interfacial tensions in three different ways that give different insights into protein interfacial activity and provoke interpretation in terms of the behavior of water at surfaces.

### General aspects of the data

Table II compiles quantitative results of this work. Contact angle parameters $\theta_a^\circ$, $\theta_a'$, $\ln C_B^{\theta_2}$ and M listed in columns 2 through 5 of Table II are the mean fitted values corresponding to final 25 $\theta_a$ curves recorded within the 60-min time frame of the TPG experiment. Listed error is standard deviation of this mean. Corresponding adhesion tensions $\tau_a^\circ$ and $\tau_a'$ (columns 6, 7) were computed from $\theta_a'$ values, respectively, with uncertainty estimates computed by propagation of error in $\theta_a$ and $\gamma_{lv}$ measurements (Methods and Materials). Maximum spreading pressure $\Pi_a^{max} \equiv (\tau_a' - \tau_a^\circ)$ (column 8) was computed directly from aforementioned $\tau_a$ values and associated uncertainty again estimated by propagation of error. Replicate protein preparations were studied for Ub, FV HSA, FXII, IgM and

$\alpha_2$-macroglobulin. Different vendors were used as a means of controlling for discrepancies that might arise from sourcing (Table I). In consideration of all sources of error ranging from solution preparation to data reduction (including purity of commercial protein preparations discussed in Ref. 25), we conclude that variation associated with manipulation and dilution of protein concentrates ($\sim$ 10 mg/mL; includes transfer losses by adsorption to pipettes, vials, and wells; slight but inevitable foaming of proteins brought into solution from powder; etc.) overwhelms $\theta_a$ measurement error discussed in the Materials and Methods and that differences between preparations or vendors were insufficient to affect basic conclusions of this work.

### Quantitative comparison of proteins and surfactants

Concentration-dependent contact angles of protein and surfactant solutions ($\theta_a$ isotherms) on methyl-terminated SAMs fell into one of two categories, identified herein as type 1 and type 2. Type 1 $\theta_a$ curves were clearly sigmoidal with distinct low- and high-concentration plateau [see, as examples, Figs. 1(A,B)] measured by $\theta_a^\circ$ and $\theta_a'$ parameters. Steady-state was apparently achieved in type 1 adsorption at-or-before 1 h drop age whereupon kinetic effects in $\theta_a$ were no longer resolvable at any concentration (less than about 1°). No semblance of a $\theta_a'$ plateau was reached at the highest concentrations studied for type 2 proteins [ubiquitin and $\alpha_2$-macroglobulin; see Fig. 1(C) for an example]. Only graphical estimates are provided in Table II for type 2 protein parameters because firm values could not be ascertained by statistical fitting procedures described in the Methods and Materials section. No attempt was made to estimate the exponential parameter M for type 2 proteins. It was not evident from this work whether these proteins would exhibit type 1 behavior if yet-higher concentrations were available for study. We note, however, that kinetic effects had fully dampened for type 2 adsorption within the interval $3500 < t < 3600$ s of the TPG experiment. This strongly suggests that steady state had in fact been achieved, but that higher solution concentrations were required to saturate the surface and achieve a verifiable $\theta_a'$ plateau. Moreover, we note that large proteins such as IgM achieved steady state over the 60-min observation interval, confirming that mass transport and adsorption kinetics could indeed be completed within the time frame of the TPG experiment, even for much larger proteins. We thus conclude that type 2 adsorption was concentration — rather than time — limited. Indeed, theoretical interpretation of protein adsorption to the LV interface suggests that surface-saturating concentrations for small proteins such as ubiquitin (10.7 kDa) exceed solubility limits,[16] explaining why a verifiable $\theta_a'$ plateau was not achieved for this protein. This same argument cannot be applied to results obtained for a molecule as large as $\alpha_2$-macroglobulin (725 kDa), however, and the outcome for this protein stands exceptional, not only to others listed in Table I but also to studies of adsorption of this protein to the LV surface.[16]

$\theta_a^\circ$ (column 2, Table II) is a measure of variability in surface-to-surface preparation procedures measured with a droplet of pure PBS in contact with the surface for 1 h. Scanning down the rows of column 2, it is apparent that $\theta_a^\circ$ data fell between 104° and 100°. Much of this variability can probably be attributed to differences in substratum hydration that gives rise to a small but clearly observable decrease in $\theta_a^\circ$ with time [see arrow annotation, Fig. 1(B) and Methods and Materials]. Adsorption of either protein or surfactant to the solid surface from aqueous solution leads to measurable, concentration-dependent decrease in $\theta_a$ to lower limit values $\theta_a'$ collected in column 3. In the case of proteins, this decrease in contact angle was quite modest, generally less than 15°, and showed little discernable trend among the proteins listed in Table I. By contrast, the surfactant reference standard SDS gave rise to about 44° decrease in $\theta_a$. Adsorption energetics are best gauged in terms of adhesion tension $\tau_a = \gamma_{lv} \cos\theta_a$ because $\tau$ is linearly related to free energy of adsorption $\Delta G_{ads}$ that simultaneously accounts for adsorption to the LV and SL surface.[6,17–19] Columns 6 and 7 of Table II collect $\tau_a^\circ$ and $\tau_a'$ parameters (corresponding to measured $\theta_a^\circ$ and $\theta_a'$) and converts these to spreading pressure $\Pi_a^{max} \equiv (\tau_a' - \tau_a^\circ)$ in column 8. Examination of $\Pi_a^{max}$ values shows that albumin and $\alpha_2$-macroglobulin exhibited the strongest biosurfactancy whereas C1q was weakest on this scale. However, from a broader perspective, it is apparent that proteins studied were more alike than dissimilar, as has been noted in adsorption to the LV surface.[16,25,28,29] Proteins clearly exhibited modest surfactancy compared to SDS for which $\Pi_a^{max} = 31$ m$N$/m. The free energy of protein adsorption to the hydrophobic surface $\Delta G_{ads}^\circ = -$ RT lnP must be commensurately modest and, based on a partition coefficient P : 150 (see Introduction), $\Delta G_{ads}^\circ = -$RT lnP $\sim -5$RT; consistent with estimates for lysozyme, myoglobin, and $\alpha$-amylase determined by hydrophobic interaction chromatography.[38]

With the above in mind, it is of interest to estimate the extent that adsorption depletes a fluid phase in contact with a hydrophobic surface because it provides a tangible sense of protein surfactancy. Adopting 2 mg/m$^2$ as a nominal protein concentration adsorbed to the surface of a hypothetical 10 $\mu$L spherical drop ($2.2 \times 10^{-5}$ m$^2$ surface area) from a surface-saturating 3 mg/mL bulk-phase composition (e.g., al-

bumin adsorbed to the LV surface as determined by neutron reflectometry),[16,26] it is evident that only 47 ng or about 0.15% of bulk-phase protein is removed by adsorption. Thus, it can be concluded that protein adsorbed from a contact-angle droplet to a hydrophobic surface does not significantly deplete the bulk fluid phase. That is to say, proteins are weak surfactants. Indeed, it may be reasonably concluded from this simple analysis that proteins do not adsorb avidly to hydrophobic surfaces, as is commonly acknowledged,[39,40] if solution depletion is used as the measure of adsorption. At the same time, however, it must be borne in mind that a partition coefficient $P \sim 150$ means that interphase concentrations expressed in mass or moles per-unit-volume (not mass or moles per-unit-surface area) are 150× bulk-phase compositions (i.e., ~ 450 mg/mL at surface saturation).[16,28] Certainly, from this point of view, proteins do adsorb avidly to a hydrophobic surface. These seemingly divergent perspectives of protein adsorption can be reconciled by recognizing that the (LV or SL) interphase is very thin, between 1 and 5 molecular layers for the proteins studied herein,[16] with a commensurately low total volume that effectively magnifies surface concentrations expressed in per-unit-volume dimensions. Thus, even though protein saturates a hydrophobic interphase at volume fractions[16] as high as one third, the total mass of protein within this interphase is sparingly small in comparison to that contained in a macroscopic volume of bulk solution.

It is of special interest to the development of hemocompatible materials that FXII did not exhibit extraordinary adsorption behavior ($\Pi_a^{max} \sim 15$ mN/m) because FXII adsorption from whole blood or plasma to procoagulant materials is thought to potentiate the intrinsic pathway of coagulation. As will be discussed subsequently, FXII surface activity is substantially mitigated by a low-physiologic concentration that does not sustain a high level of interfacial activity.

## Graphical interpretation of results

Time-and-concentration-dependent $\theta_a$ for the anionic surfactant SDS, purified protein HSA (Fraction V, FV HSA), and $\alpha_2$-macroglobulin are compared in Figure 1 in both three-dimensional (3D, $\theta_a$ as a function of time and concentration) and two-dimensional (2D, $\theta_a$ as a function concentration at specified times) representations. Examining first 3D and 2D representations of SDS interfacial activity [Fig. 1(A)] which serves as a reference compound, it was observed that the $\theta_a$ curve was sigmoidal in shape, with a well-defined low-concentration asymptote $\theta_a^{\circ}$ and a high-concentration asymptote $\theta_a'$ characteristic of type 1 adsorption. In this latter regard, SDS and HSA exhibited similar concentration-limiting behavior [compare Fig. 1(A,B) that is typically interpreted as formation of a critical micelle concentration (CMC), at least for surfactants.[41] This article provides no evidence of micelles, for either proteins or surfactants, and so only acknowledges a limiting behavior at which further increase in solute concentration did not measurably change $\theta_a$. Unlike SDS, however, adsorption/mass transfer kinetics significantly affected early-time $\theta_a$ measurements of HSA solutions, although steady state was achieved well before the final observation time at 3600 s. Kinetic effects were even more pronounced for large proteins such as $\alpha_2$-macroglobulin [Fig. 1(C)] for which type 2 adsorption behavior was observed. Thus, Figure 1 captures the significant adsorption trends quantified in Table II.

## Scaled interfacial activity

Figure 2 traces the sequential interpretation of steady-state, concentration-dependent $\theta_a$ data [Fig. 2(A), observed at 1 h drop age] in terms of $\tau_a$ [Fig. 2(B)] and spreading pressure $\Pi_a$ [Fig. 2(C)] isotherms for the proteolytic enzyme thrombin (blood factor FIIa). Smooth curves through the data (see Methods and Materials) provide guides to the eye. Figure 3(A,B,C) compare $\Pi_a$ curves for proteins selected from Table I to cover the full range of molecular weight (MW) studied in this work. Concentration is scaled in three different ways in Figure 3 for direct comparison; by weight [Fig. 3(A)], molarity [Fig. 3(B)], and ratio-to-physiological concentration, $C_P$ [Fig. 3(C)]. Only smoothed curves corresponding to steady-state (equilibrium) are shown for the sake of clarity, but representative $\theta_a$, $\tau_a$, and $\Pi_a$ curves with authentic data are amply illustrated in Figures 1 and 2. The following discusses results of each scaling method in order of appearance on Figure 3. These different scaling methods sharpen general impressions about the energetics of protein adsorption that are particularly pertinent to the controlling role of water in protein adsorption discussed in the Introduction.

Figure 3(A) compares $\Pi_a$ curves with $C_B$ expressed in parts-per-trillion (i.e., PPT, grams solute/$10^{12}$ g solvent, so that the ln $C_B$ scale has positive values at all concentrations). Weight scaling is applicable to purified proteins, protein mixtures, and surfactants alike, permitting comparison of interfacial activity on a single concentration axis.[17–19] Two features are readily apparent from Figure 3(A). First, the dynamic range of $\Pi_a \sim 20$ m$N$/m is consistent with weak surfactancy, as discussed in the previous section, and is similar to that observed for these proteins at the LV surface ($15 < \Pi_a < 30$ m$N$/m). Second, $\Pi_a$ lies within a relatively narrow 5 m$N$/m band for this diverse set of proteins

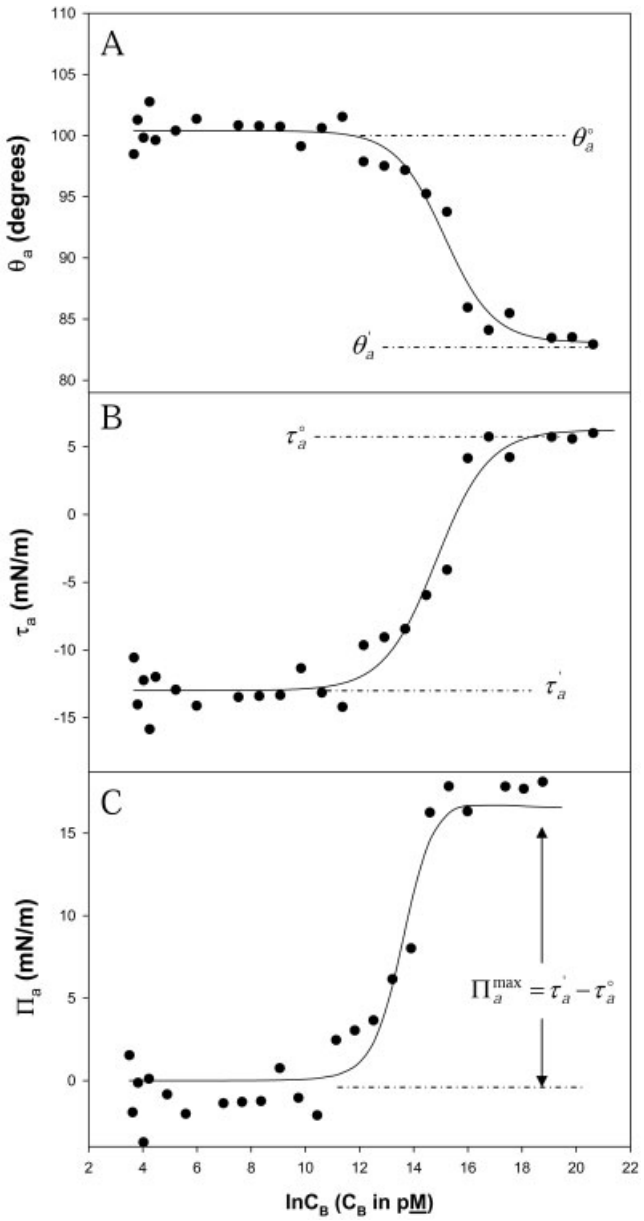


**Figure 2.** Sequential interpretation of a steady-state (3600 s drop age) contact angle adsorption isotherm for thrombin (FIIa). Panel A, advancing contact angles, $\theta_a$; panel B, advancing adhesion tension, $\tau_a$; panel C, advancing spreading pressure $\Pi_a$. Smoothed curves through the data are guides to the eye. Annotations identify low- and high-concentration asymptotes for contact angles ($\theta_a^\circ$, $\theta_a'$), adhesion tensions ($\tau_a$, ($\tau_a$) respectively, and maximum spreading pressure $\Pi_a$ that are used to characterize isotherms (Table II).

(with MW spanning nearly three orders of magnitude; see Table I). Thus, it is evident from Figure 3(A) that, on a weight basis, proteins exhibit quite similar SL interfacial activity, mirroring the general experience with these proteins at the LV surface.[25] Bearing in mind the great range in MW spanned by proteins in Figure 3, it is reasonable to conclude that commensurate variability in protein structure does not confer widely varying SL interfacial activity; at least not in comparison to the full range available to ordinary surfactants.

However convenient weight scaling may be, it is nevertheless true that free energy and stoichiometry scale on a molar basis. Thus, for the purpose of better understanding interfacial energetics, it is useful to

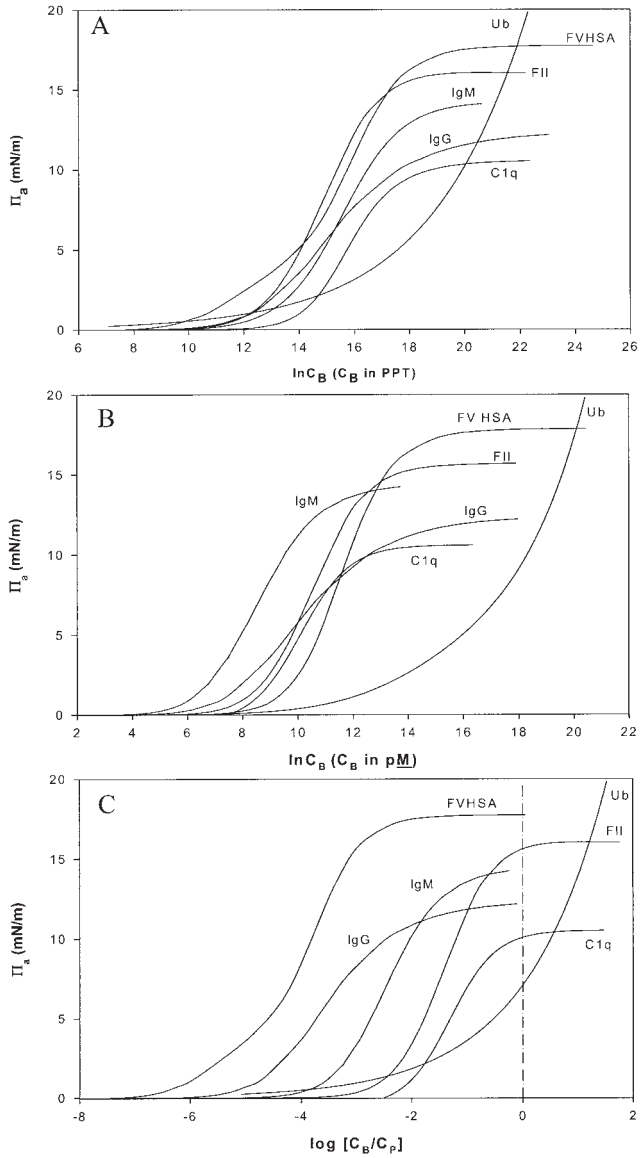


**Figure 3.** Spreading pressure $\Pi_a$ isotherms scaled three different ways for selected proteins spanning three decades in molecular weight — by natural logarithmic weight-volume (panel A), picomolarity (panel B), and logarithmic (base 10) ratio-to-physiological concentration (panel C). Smooth curves are guides to the eye. Protein interfacial activity appears more similar than dissimilar when viewed on a weight basis but diversity among proteins becomes more apparent when scaled on a molar or ratio-to-physiological concentration. Physiologic scaling (panel C) shows that FV HSA, IgG, and IgM (preparation 1, Table I) were fully surface active at-and-below physiological concentrations whereas C1q, FII, and Ub required nearly 2× concentration to achieve maximum spreading pressure.

express bulk concentration $C_B$ in molar units. We have chosen to express solute dilution $C_B$ in picomoles/L (i.e., picomolarity, p*M*, $10^{-12}$ moles solute/L solution so that the $\ln C_B$ scale has positive values for all dilutions) for solutes with a known (nominal) MW. This approach is applicable to purified proteins and surfactants but not to chemically undefined protein mixtures such as plasma and serum. Variability in interfacial activity among the diverse purified proteins reported in Figure 3 is much more evident on a molar than weight basis [compare Fig. 3(A) to Fig. 3(B)]. Of course, molar scaling does not alter observations regarding the range of $\Pi_a$ mentioned above, but it does effectively expand the concentration axis by moving higher-MW proteins (such as IgM) to the left and lower-MW proteins (such as albumin and ubiquitin) to the right. It is evident from Figure 3(B) that high-MW proteins reduce $\Pi_a$ at lower molarity than low-MW proteins, again repeating a general observation made at the LV surface for these proteins. The inference taken from Figure 3(B) is that protein concentration required to reduce $\Pi_a$ to a specified value decreases with MW in a manner loosely consistent with the addition of a generic amino-acid-building-block having an average amphilicity that increases MW but does not radically change protein interfacial activity. Otherwise, if MW increased by addition of amino-acid-building-blocks with highly variable amphilicity, then $\Pi_a$ would be expected to be a much stronger function of protein MW than is observed in Figure 3(B). Thus, it appears that molar variability in $\Pi_a$ is achieved by aggregating greater mass of similar amphiphilic character, as opposed to accumulating greater amphilicity with increasing MW.

Weight and molar scaling are very useful experimental and conceptual constructs that may turn out to have little direct relevance to the *in vivo* biological response to materials because these scales do not account for the widely varying natural abundance of the many different proteins comprising the mammalian proteome.[42] Thus, for the purpose of better understanding protein interfacial activity within a physiologic context, we have found it useful to ratio $C_B$ to nominal (mean) physiological concentration $C_P$ and express $C_B/C_P$ on a logarithmic scale [$\log(C_B/C_P)$]. In this way, the physiologic condition can be readily identified at $\log(C_B/C_P) = 0$ with more-dilute-protein solutions lying to the left [negative $\log(C_B/C_P)$ values] and more-concentrated solutions lying to the right [positive $\log(C_B/C_P)$ values; see dashed vertical line on Fig. 3(C)]. This approach is applicable to purified proteins for which humoral or cellular concentrations are known. Thus, Figure 3(C) reveals a different kind of diversity in protein interfacial activity than discussed above in reference to weight or molar scales. Certain proteins, notably albumin, IgG and IgM, produced the full $\Pi_a^{max}$ range well below physiologic concentration ($\Pi_a$ data lies substantially to the left of $\log(C_B/C_P) = 0$). By contrast, C1q and prothrombin (FII) required full physiological concentration to express $\Pi_a^{max}$ whereas ubiquitin was not fully surface active at-and-well-above physiologic concentration. Again, these results closely correspond to the behavior noted at the LV surface. And just as observed at the LV surface, only a limited portion of the available $\Pi_a^{max}$ range was exhibited by blood factor XII ($\Pi_a$ data lie to the right of $\log(C_B/C_P) = 0$, as will be discussed separately below in reference to Figure 4 because this has special significance in blood coagulation. Thus, it appears that $\log(C_B/C_P)$ is a pragmatic scaling of interfacial activity with relevance to biomedical materials that reveals concentration-driven diversity in interfacial activity observed among humoral and cellular proteins.

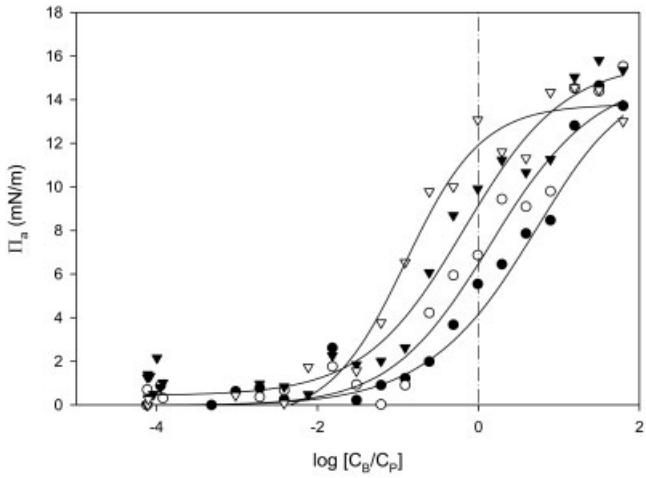


**Figure 4.** Spreading pressure $\Pi_a$ isotherms of blood factor FXII (preparation 1, Table I), scaled as a ratio-to-physiological concentration. Smooth curves at 0.25, 900, 1800, and 3594 s drop age illustrate FXII adsorption kinetics. FXII is weakly surface active at physiologic concentrations (see Fig. 3 for comparison to other proteins such as FVHSA, IgG). Note that maximum spreading pressure was achieved only at two decades of concentration higher than physiologic concentration.

Figure 4 summarizes results obtained for blood factor FXII. Activation of FXII by contact/adsorption to procoagulant surfaces is thought to potentiate the intrinsic pathway of blood coagulation (see Refs. 43, 44 and citations therein). Thus, understanding interfacial activity of FXII is important toward a full appreciation of the contact activation mechanism[45–47] and anticoagulation as well.[48] Figure 4 is prepared in basically the same format as Figure 3(C) except that $\Pi_a$ curves here correspond to different observation times up to 1 h drop age and demonstrates that FXII $\Pi_a^{max}$ was not achieved at physiological concentrations. Moreover, $\Pi_a^{max}$ was achieved only after long equilibration times ($> 1800$ s). These adsorption kinetics must be interpreted in terms of the blood-plasma-coagulation pro-

cess that can be complete within 300 s or so when plasma is saturated with high-surface-area procoagulants.[46] Results obtained with purified FXII are thus seemingly inconsistent with the traditional biochemical mechanism of contact activation of blood plasma coagulation that asserts rapid FXII adsorption onto hydrophilic procoagulant surfaces. FXII adsorption, and FXIIa desorption for that matter, must occur in the presence of overwhelming concentrations of other blood proteins, notably albumin and IgG that this work demonstrates to be much more surface active on both molar and physiological-concentration scales [Fig. 3(B,C)]. Furthermore, we note that FXII adsorption to the SL interface is not rapid relative to other proteins such as albumin, as might be expected for a protein with putatively enhanced interfacial activity. Although mechanisms of adsorption to hydrophilic (efficient procoagulant) surfaces are not necessarily the same as those leading to adsorption to hydrophobic (inefficient procoagulant) surfaces, it is the general experience that much more protein is adsorbed to hydrophobic surfaces.[39,47] On this basis, we expect that FXII would exhibit even less adsorption to hydrophilic procoagulants than we observe at the hydrophobic SL surface within a time-frame relevant to coagulation. All taken together, these studies of FXII adsorption to the hydrophobic SL and LV interfaces support our contention that FXII does not adsorb directly onto hydrophilic procoagulant surfaces in a manner that displaces water (surface dehydration) and that contact activation of FXII → FXIIa occurs by some process other than suggested by the traditional mechanism.[46–48]

## CONCLUSIONS

Concentration-dependent contact angles $\theta_a$ of buffered-protein solutions on methyl-terminated self assembled monolayer (SAM) surfaces have been measured for selected globular-blood proteins spanning three decades in molecular weight (MW). Observed protein $\theta_a$ was reduced by no more than 15° at maximum protein concentrations (~10 mg/mL). Adsorption energetics were interpreted in terms of adhesion tension $\tau_a = \gamma_{lv} \cos\theta_a$ and spreading pressure $\Pi_a = (\tau_a - \tau_a^\circ)$ adsorption isotherms, where $\gamma_{lv}$ is concentration-dependent liquid–vapor (LV) interfacial tension of the fluid phase, $\tau_a'$ is the adhesion tension corresponding to minimum contact angle $\theta_a'$, and $\tau_a^\circ$ is the adhesion tension of pure buffer. Results closely mirrored that reported in a companion paper published in this journal describing protein adsorption to the hydrophobic aqueous-buffer/air (liquid–vapor, LV) interface.[25] On this basis, it is concluded that the physical chemistry of protein adsorption to the solid–liquid (SL) interface is not remarkably different than that controlling protein adsorption to the LV interface. In particular, it was found that maximum spreading pressure fell within a relatively narrow $10 < \Pi_a^{max} < 20$ m$N$/m band for all proteins studied. Results confirm that proteins are, in general, weak surfactants in comparison to synthetic detergents (represented herein by the surfactant reference compound sodium dodecyl sulfate, SDS). The free energy of adsorption to hydrophobic surfaces is thus found to be quite modest ($\Delta G_{ads}^\circ \sim -5RT$) and the total protein adsorbed from a contact-angle droplet a small percentage of the total available in solution. However, adsorbed concentrations in mass or moles per-unit-volume are surprisingly large (~ 450 mg/mL)[6,16,28] because adsorbate collects within an thin (SL or LV) interphase, arguably no more than a few protein molecular layers thick.

Three different methods of scaling $\Pi_a$ isotherms were explored: weight, molarity, and ratio-to-physiologic concentration. On a weight basis, proteins among the group studied appeared more similar than dissimilar, especially when viewed from the perspective of the full range available to synthetic surfactants. We interpret this observation to mean that there is insufficient amphiphilic diversity (variation in the interaction energetics with water) among the proteins studied to support wide-ranging interfacial activity at the hydrophobic SL interface, even though protein composition varied significantly among proteins studied. Molar scaling revealed that SL interfacial activity followed a progression in MW, with the concentration required to reach a specified $\Pi_a$ value decreasing with increasing MW. This progression in MW is interpreted to mean that molar variability in $\Pi_a$ is achieved by aggregating greater mass of similar amphiphilic character (blocks of amino acids), as opposed to accumulating greater amphilicity with MW. The significance of this observation is that it suggests that the structural variability that confers profoundly different bioactivity does not greatly affect interaction energetics in water that drive adsorption to the LV interface. Scaling interfacial activity to physiological concentration revealed that certain proteins, such as albumin and IgG, achieved $\Pi_a^{max}$ at and well below physiologic concentration whereas others, notably blood factor XII (Hageman factor), required concentration by almost two-fold above the nominal-physiologic concentration to express the full range of $\Pi_a^{max}$characteristic of this protein.

In summary, results reported herein support the overall conclusion that combinations and permutations of the 20 naturally occurring amino acids comprising the primary sequence of mammalian proteins is insufficient to support widely varying interfacial activity at hydrophobic surfaces (LV or SL), no matter how these sequences happen to fold into higher-order structure.[25] Furthermore, we contend that protein con-

centration, not diversity in molecular structure, is the significant energetic driver of adsorption to hydrophobic surfaces. The overarching interpretation is that water plays a dominant, controlling role in the adsorption of globular blood proteins to hydrophobic surfaces and that the mechanism of protein adsorption can be quite comprehensively understood from this perspective.

Outcomes of this work are in general agreement with other investigations of the interfacial energetics of protein adsorption. In particular, the pioneering work of Tripp, Magda, and Andrade[49] revealing that "...mesoequilibrium surface tension [of 8 globular proteins]...did not vary greatly between different proteins..." is relevant to this investigation. The term *mesoequilibrium* was wisely applied by Tripp and colleagues because, in general, it is technically challenging to unambiguously prove fully reversible adsorption (or thermodynamic reversibility of any process for that matter). And in the particular case of proteins, there is the expectation from a burgeoning literature base that proteins denature over time (see Ref. 50 and citations therein). Denaturation can include changes in molar free volume/interfacial area, loss of higher-order structure with concomitant change in specific bioactivity, and irreversible adsorption. Of course, tensiometric methods applied by Tripp and colleagues and us are effectively blind to these molecular processes, except insofar as denaturation may lead to time-varying interfacial tensions and contact angles. Our measurements achieved, or asymptotically approached, a well-defined steady state within the hour observation window applied, suggesting that putative denaturation processes either had an insignificant impact on results or occurred significantly faster/slower than the time frame of experimentation. Given the similarity in adsorption energetics to hydrophobic LV and SL surfaces among the broad array of proteins studied (including those of Tripp et al.), and the general expectation that denaturation is a slow process, we are inclined to conclude that either denaturation did not significantly affect results (perhaps accounting for small-but-measurable differences among proteins) or the denaturation effect was astonishingly similar among very different proteins. With regard to irreversible adsorption, we note that experiments examining competitive adsorption between albumin and IgM at the LV surface demonstrated protein displacement (Vroman effect) that followed a simple mass-balance exchange,[28] strongly suggesting that neither albumin nor IgM was irreversibly adsorbed to this surface.

Even in view of the similarity among studies of the interfacial energetics of protein adsorption to hydrophobic surfaces, it is difficult to fully reconcile our findings with all other previous investigations of protein adsorption. But then it is also challenging to find substantive commonality within and among this prior art,[6] let alone extend its margins to embrace new findings. Thus, there should be little surprise that results reported herein may seem exceptional relative to certain particular studies selected from this expansive literature base. In this connection, it seems useful to step back from the details momentarily and point out that relating mass to energy inventories of protein adsorption will require more than casual comparison of experimental results. For this purpose, a theory of protein adsorption is required. And until such a theory is available, comparison of mass measurements (by solution depletion, gravimetry, or spectroscopy, for example) to interfacial energetics (by calorimetry, chromatography, or tensiometry, for example) should be made with due caution.

The authors gratefully acknowledge the assistance of Dr. Roger Woodward in instrument design and implementation.

## References

1. Horbett T. Protein adsorption on biomaterials. In: Cooper SL, Peppas NA, Hoffman AS, Ratner BD, editors. Biomaterials: interfacial phenomena and applications. Washington, DC: American Chemical Society; 1982. p 234–243.
2. Ratner BD, Castner DG, Horbett TA, Lenk TJ, Lewis KB, Rapoza RJ. Biomolecules and surfaces. J Vac Sci Technol 1990; 8:2306–2317.
3. Horbett TA. Principles underlying the role of adsorbed plasma proteins in blood interactions with foreign materials. Cardiovac Pathol 1993;2:137S–148S.
4. Malmsten M, editor. Biopolymers at interfaces. New York: Marcel Dekker; 1998. 656 p.
5. Horbett TA. Biological activity of adsorbed proteins. In: Malmsten M, editor. Biopolymers at interfaces. New York: Marcel Dekker; 1998. p 393–413.
6. Vogler EA. Structure and reactivity of water at biomaterial surfaces. Adv Colloid Interface Sci 1998;74:69–117.
7. Vogler EA. Water and the acute biological response to surfaces. J Biomater Sci Polym Edn 1999;10:1015–1045.
8. Vogler EA. Role of water in biomaterials. In: Ratner B, Hoffman A, editors. Biomaterials science: an introduction to materials in medicine. San Diego: Elsevier Academic Press; 2004.
9. Vogler EA. Biological properties of water. In: Morra M, editor. Water in biomaterials surface science. New York: Wiley; 2001. p 4–24.
10. Vogler EA. How water wets biomaterials. In: Morra M, editor. Water in biomaterials surface science. New York: Wiley; 2001. p 269–290.
11. Andrade JD, Hlady V. Protein adsorption and materials biocompatibility: a tutorial review and suggested mechanisms. Adv Polym Sci 1986;79:3–63.
12. Nandi N, Bagchi B. Dielectric relaxation of biological water. J Phys Chem B 1997;101:10954–10961.
13. Cho EC, Kim YD, Cho K. Effect of bound water structure on the protein substrate interaction and protein adsorption behavior. Polymer Preprints 2003;44:173–174.
14. Garcia C, Anderson JM, Barenberg SA. Hemocompatibility: effect of structured water. Trans Am Soc Intern Organs 1980; 26:294–298.

15. Pollack GH. Cells, gels, and the engines of life: a new, unifying approach to cell function. Seattle: Ebner & Sons; 2001.
16. Krishnan A, Siedlecki C, Vogler EA. Traube-rule interpretation of protein adsorption to the liquid–zapor Interface. Langmuir 2003;19:10342–10352.
17. Vogler EA. Interfacial chemistry in biomaterials science. In: Berg J, editor. Wettability. New York: Marcel Dekker; 1993. p 184–250.
18. Vogler EA. Practical use of concentration-dependent contact angles as a measure of solid-liquid adsorption I: theoretical aspects. Langmuir 1992;8:2005–2012.
19. Vogler EA. Practical use of concentration-dependent contact angles as a measure of solid-liquid adsorption II: experimental aspects. Langmuir 1992;8:2013–2020.
20. Vogler EA, Martin DA, Montgomery DB, Graper JC, Sugg HW. A graphical method for predicting protein and surfactant adsorption properties. Langmuir 1993;9:497–507.
21. Vogler EA. On the origins of water wetting terminology. In: Morra M, editor. Water in biomaterials surface science. New York: Wiley; 2001. p 150–182.
22. Crystall B, Rumbles G, Smith T, Phillips D. Time resolved evanescent wave induced fluorescent measurements of surface adsorbed bovine serum albumin. J Colloid Interface Sci 1993; 155:247–250.
23. Walton AG, Maenpa FC. Application of fluorescence spectroscopy to the study of proteins at interfaces. J Colloid Interface Sci 1979;72:265–278.
24. Xu X-HN, Yeung ES. Long-range electrostatic trapping of single-protein molecules at a liquid–solid interface. Science 1998; 281:1650–1653.
25. Krishnan A, Sturgeon J, Siedlecki CA, Vogler EA. Scaled interfacial activity of proteins at the liquid–vapor interface. J Biomed Mater Res 2004;68A:544–557.
26. Lu JR, Su TJ, Penfold J. Adsorption of serum albumins at the air/water interface. Langmuir 1999;15:6975–6983.
27. Zhou C, Friedt J-M, Angelova A, Choi K-H, Laureyn W, Frederix F, Francis LA, Campitelli A, Engelborghs Y, Borghs G. Human immunoglobulin adsorption investigated by means of quartz crystal microbalance dissipation, atomic force microscopy, surface acoustic wave, and surface plasmon resonance techniques. Langmuir 2004;20(4):5870–5878.
28. Krishnan A, Siedlecki CA, Vogler EA. Mixology of protein solutions and the vroman effect. Langmuir 2004;20:5071–5078.
29. Krishnan A, Wilson A, Sturgeon J, Siedlecki CA, Vogler EA. Liquid-vapor interfacial tension of blood plasma, serum and purified protein constituents thereof. Biomaterials 2005;26: 3445–3453.
30. Putnam FW. Alpha, beta, gamma, omega - the roster of the plasma proteins. In: Putnam FW, editor. The plasma proteins: structure, function, and genetic control. New York: Academic Press; 1975. p 58–131.
31. Allara DL, Nuzzo RG. Spontaneously organized molecular assemblies. 2. Quantitative infrared spectroscopic determination of equilibrium structures of solution-adsorbed n -alkanoic acids on an oxidized aluminum surface. Langmuir 1985;1:52–66.
32. Nuzzo RG, Allara DL. Adsorption of bifunctional organic disulfides on gold surfaces. J Am Chem Soc 1983;105:4481–4483.
33. Nuzzo RG, Fusco FA, Allara DL. Spontaneously organized molecular assemblies. 3. Preparation and properties of solution adsorbed monolayers of organic disulfides on gold surfaces. J Am Chem Soc 1987;109:2358–2368.
34. Nuzzo RG, Dubois LH, Allara DL. Fundamental studies of microscopic wetting on organic surfaces. 1. Formation and structural characterization of a self-consistent series of polyfunctional organic monolayers. J Am Chem Soc 1990;112:558–569.
35. Porter MD, Bright TB, Allara DL, Chidseyi CED. Spontaneously organized molecular assemblies. 4. structural characterization of n-alkyl thiol monolayers on gold by optical ellipsometry, infrared spectroscopy, and electrochemistry. J Am Chem Soc 1987;109:3559–3568.
36. Krishnan A, Liu Y-H, Cha P, Allara DL, Vogler EA. An evaluation of goniometric methods. J Colloid Interface Sci 2005;43: 95–98.
37. Krishnan A, Liu Y-H, Cha P, Allara DL, Vogler EA. Interfacial energetics of globular-blood protein adsorption to a hydrophobic solid-water surface. J Roy Soc Interface 2005. In review.
38. Wen-Yih Chen H-MH, Chien-Chen Lin, Fu-Yung Lin, Yu-Chia Chan. Effect of temperature on hydrophobic interaction between proteins and hydrophobic adsorbents: studies by isothermal titration calorimetry and the van't Hoff equation. Langmuir 2003;19:9395–9403.
39. Hoffman AS, Ratner BD. Nonfouling surfaces. In: Ratner B, Hoffman A, editors. Biomaterials science: an introduction to materials in medicine. San Diego: Elsevier Academic Press; 2004.
40. Horbett TA. The role of adsorbed proteins in tissue response to biomaterials. In: Ratner B, Hoffman A, editors. Biomaterials science: an introduction to materials in medicine. San Diego: Elsevier Academic Press; 2004.
41. Rosen MJ. Surfactants and interfacial phenomena. New York: Wiley; 1978. 304 p.
42. Anderson NL, Anderson NG. The human plasma proteome: history, character, and diagnostic prospects. Molec Cell Proteo 2002;1:845–867.
43. Mitropoulos KA. The levels of FXIIa generated in hyman plasma on an electronegative surface are insensitive to wide variation in the concentration of FXII, prekallikrein, high molecular weight kininogen or FXI. Thromb Haemost 1999;82: 1033–1040.
44. Mitropoulos KA. High affinity binding of factor FXIIa to an electronegative surface controls the rates of factor XII and prekallikrein activation in vitro. Thromb Res 1999;94:117–129.
45. Zhuo R, Miller R, Bussard KM, Siedlecki CA, Vogler EA. Procoagulant stimulus processing by the intrinsic pathway of blood plasma coagulation. Biomaterials 2005;26:2965–2973.
46. Vogler EA, Graper JC, Harper GR, Lander LM, Brittain WJ. Contact activation of the plasma coagulation cascade. 1. Procoagulant surface energy and chemistry. J Biomed Mater Res 1995;29:1005–1016.
47. Vogler EA, Graper JC, Sugg HW, Lander LM, Brittain WJ. Contact activation of the plasma coagulation cascade. 2. Protein absorption on procoagulant surfaces. J Biomed Mater Res 1995;29:1017–1028.
48. Vogler EA, Nadeau JG, Graper JC. Contact activation of the plasma coagulation cascade. 3. Biophysical aspects of thrombin binding anticoagulants. J Biomed Mater Res 1997;40:92–103.
49. Tripp BC, Magda JJ, Andrade JD. Adsorption of globular proteins at the air/water interface as measured via dynamic surface tension: concentration dependence, mass-transfer considerations, and adsorption kinetics. J Colloid Interface Sci 1995; 173:16–27.
50. Birdi KS. Lipid and biopolymer monolayers at liquid interfaces. New York: Plenum Press; 1989. 325 p.